ERROR CONTROL CODING FOR SATELLITE AND SPACE COMMUNICATIONS

Final Technical Report

to

NASA

Goddard Space Flight Center
Greenbelt, Maryland

Grant Number NAG 5-778

Costas N. Georghiades
Principle Investigator
(acting for Shu Lin)
Department of Electrical Engineering Department
Texas A&M University
College Station, Texas 77843

July 28, 1987

CONTENTS

I. INTRODUCTION

This is the final report for Nasa grant NAG 5-778 entitled "Error Control Coding for Satellite and Space Communications". In this report we describe in detail the new results obtained since the last submitted report in March of 1987 but only briefly describe the results obtained previously. The summary of previous results is given in section III in terms of reports and preprints of submitted papers.

The overall research goals for this grant have been attained. In the latter part of the research which started in January '87 when I took over from Professor Shu Lin, I have mainly concentrated on problems encoutered in optical communication systems for satellite and space communications. Here, some interesting results have been obtained, but more research is needed in the future on the topic.

II. NEW RESULTS

This section contains a detailed description of the technical results obtained since the last technical report was submitted to NASA on March 25. These results are reported in the form of a paper which has recently been submitted for publication in the IEEE transactions on communications.

SOME IMPLICATIONS OF TCM FOR OPTICAL DIRECT-DETECTION CHANNELS *

by

Costas N. Georghiades
Electrical Engineering Department
Texas A&M University
College Station, Texas 77843

ABSTRACT

We consider the optical direct detection channel and show how simple trellis coded modulation (TCM) can be used to improve performance or increase throughput (in bits per second) without a bandwidth expansion and no performance loss. In fact, a modest performance gain can be achieved. Although the approach can be used with other signal constellations, we concentrate on signals derived from the pulse-position modulation (PPM) format by allowing overlap. Theoretical motivation for using this signal set, known as overlapping PPM (OPPM), was recently given by Bar David et al who showed a capacity gain when overlap is introduced.

* This research was supported by NASA grant No. NAG 5-778

I. INTRODUCTION

Increasing system throughput (bits per second) in general involves either decreasing the symbol duration or increasing the number of signals in the signal space. The first approach results in an unavoidable increase in the required system bandwidth since the same number of signal dimensions must fit in a smaller time interval. The second approach may or may not result in a bandwidth expansion depending on whether the dimensionality of the signal space is increased or not. In the latter case, the incurred penalty is an increase in error-probability since signals are now closer together. Applying conventional coding to improve performance will result in an increase in the required bandwidth which may not be available.

In this paper, we apply the ideas introduced by Ungerboeck [1] in order to increase throughput at no penalty in either bandwidth expansion or performance degradation. Specifically, we are interested in doubling the throughput at no cost in bandwidth or performance. The approach we follow is to introduce enough new signals in the signal space to triple the number of bits per symbol, while keeping the dimensionality of the signal space the same to avoid bandwidth expansion. We then sacrifice some of the throughput gain using a trellis code over the expanded signal set in order to improve performance. We do this for the optical direct-detection channel and consider both the background noise case as well as the quantum-limited case where the only noise is the self-noise of the signal. The direct-detection optical channel is well modeled by Poisson statistics, under which the output of the channel is a Poisson process with intensity $(\lambda_s(t) + \lambda_n)$. Here, $\lambda_s(t)$ is the mean rate in photons per second due to the signal impinging on the photodetector and λ_n is the noise intensity, due to background and/or detector dark currents; λ_n is zero for the quantum-limited channel.

In the analysis that follows we consider overlapping pulse-position modulation (OPPM) signals which, as the name implies, allow overlap between pulse positions, in contrast to the usual orthogonal PPM. The motivation for using this signal format is given by Bar David et al [2] who showed that the capacity of the optical channel increases compared to orthogonal PPM when overlap is allowed. Moreover, it was noted in [2] that most of

the capacity gain can be achieved with a small overlap for low signal levels, as measured by the average number of photons per slot. Another advantage of OPPM is that, like PPM, it involves equal energy signals and has a low duty-cycle. The latter consideration is important due to the average power limit imposed on optical communication systems by the laser and is one of the reasons PPM is preferred over on-off keying (OOK). A more detailed description of OPPM is given in the following.

In section II we derive uncoded error-probability expressions for OPPM for both the quantum-limited as well as the background noise case. Section III contains examples of how TCM can be applied to the optical channel to increase throughput or improve performance and analysis of the coded error-probability. Finally section IV contains some conclusions.

II. OVERLAPPING PPM

A. The Model

Under OPPM a symbol interval of T seconds is subdivided into QN subintervals of equal duration τ seconds. Information is conveyed by the position of a pulse of duration $T' = N\tau$ seconds in one of the first J times $t_k = (k-1)\tau$, $k = 1, 2, ..., J$; here $t_1 = 0$ is the start of a symbol interval. It is clear that J is related to Q and N by

$$J = N(Q-1) + 1 . \tag{1}$$

As an example, figure 1 shows pictorially the $J = 4$ OPPM signals corresponding to $Q = 2$ and $N = 3$. Following the terminology in [2], we will refer to N as the *index of overlap.* Notice that Q is the alphabet size of the PPM signal set with no overlap ($N = 1$) and that by allowing overlap between pulses we have increased the number of signals from Q to J. The bandwidth of the OPPM signal set can be easily seen to be the same as that for Q-ary PPM since the signal pulse duration and the number of dimensions (Q) are the same in both cases. On the other hand, however, the extended signal set is not orthogonal anymore, which implies worse performance. Moreover, an increased burden is put on the synchronization system which must now provide better time resolution. In the analysis that follows we will assume that synchronization is either perfectly achieved or achieved to such a degree that its effects on performance are negligible.

As a demonstration of the throughput advantages of OPPM compared to orthogonal PPM let us find the maximum throughput achieved by each when a bandwidth limit B_L is imposed on a system. Measuring bandwidth by the reciprocal of the signal pulse duration, it is easily found for PPM that the throughput r in nats per second is bounded by

$$r \leq B_L \frac{\ln(Q)}{Q} \leq \frac{B_L}{2} \ln(2). \tag{2}$$

For OPPM we have

$$r \leq B_L \frac{\ln[N(Q-1)+1]}{Q} \leq \frac{B_L}{2} \ln(N+1). \tag{3}$$

Equality on the right-most inequalities in (2) and (3) is achieved when $Q = 2$, which implies that when throughput is a prime consideration, there is an advantage in limiting the PPM alphabet size to $Q = 2$. A simple comparison between (2) and (3) shows the throughput advantage of OPPM over PPM.

The uncoded error-probability performance of a $Q = 4$ OPPM system was previously studied in [3] for a suboptimal receiver that implemented threshold detection to make symbol decisions. The authors in [3] noted that the increased throughput was obtained at a large cost in performance. In this paper we derive similar results for the performance of optimal receivers and show with specific examples, using trellis coded modulation (TCM) with simple codes, that performance loss can be avoided even when throughput is doubled with no bandwidth increase. Before we proceed further, we note that our results are not meant to compete with those reported by McEliece [4] and Massey [5] in terms of error-probability. Such a comparison will be unfair since their coding schemes exploit an appreciable bandwidth expansion in order to increase communication efficiency in bits per photon.

B. Uncoded Error-Probability

Under the Poisson channel assumption, the sufficient statistic can be easily derived to be the number of photons N_k, $k = 1, 2, ..., J$, observed in each of the J subintervals corresponding to pulse-positions. These counts are Poisson distributed with mean $(\lambda_s + \lambda_n)T'$

when a signal pulse is present and $\lambda_n T'$ otherwise. The receiver makes a decision by choosing the symbol interval with the largest number of counts. In case of symbols with equal counts, a random choice is made among those symbols.

We first concentrate on the quantum-limited case, $\lambda_n = 0$. In this case it can be easily seen that the sufficient statistic simplifies to the binary vector $\mathbf{x} = (x_1, x_2, ..., x_{NQ})$ where

$$x_i = \begin{cases} 1, & \text{if } n_i > 0; \\ 0, & \text{otherwise;} \end{cases} \tag{2}$$

here, n_i, $i = 1, 2, \cdots, NQ$, is the number of counts in the i-th τ-second subinterval dividing T. With no background noise, the channel becomes an erasure channel (not binary) with an erasure probability in each pulsed τ-second interval equal to

$$\epsilon = \exp(-\lambda_s \tau). \tag{3}$$

. This means that $Pr[x_i = 0]$ equals ϵ when a signal pulse is present in the $i-th$ τ-second subinterval and it equals one otherwise.

Leaving the details of the derivations for appendix A, the uncoded error-probability can be shown to be

$$P(\epsilon) = 1 - \frac{1}{J}[2P_1 + (J-2)P_2] \tag{4}$$

where

$$P_1 = (1 - \epsilon)[1 + \sum_{k=1}^{N-1} \frac{\epsilon^k}{k+1}] + \frac{\epsilon^N}{J} \tag{5}$$

$$P_2 = (1 - \epsilon)^2 + (1 - \epsilon)(2 - \epsilon) \sum_{k=1}^{N-1} \frac{\epsilon^k}{k+1} + \frac{\epsilon^N}{J} + \frac{\epsilon^N}{N}(1 - \epsilon). \tag{6}$$

Defining by μ the number of signal photons per *information* nat, we have $\lambda_s T' = \mu R \ln(J)$ photons per channel use (cu) where R is the number of information symbols per channel symbol. Remembering that $T' = N\tau$, we have for uncoded systems

$$\epsilon = \exp(-\frac{\mu}{N} \ln(J)). \tag{7}$$

A brief check indicates that equation (4) reduces to the right equation for the Q-ary PPM case when $N = 1$.

When background noise is present, the following bound on error-probability is derived in appendix B for uncoded systems.

$$P(e) \leq \frac{1}{J}\sum_{i=1}^{N} a(i)Q_1[\sqrt{\frac{2i\lambda_n T'}{N}}, \sqrt{\frac{2i[\lambda_n T' + \mu \ln(J)]}{N}}] \leq \frac{1}{J}\sum_{i=1}^{N} a(i)\exp[-i\gamma] \qquad (8)$$

where $Q_1(\ ,\ )$ is Marcum's Q function [9],

$$a(i) = \begin{cases} 2(J - i),\ i = 1, 2, \cdots, (N-1); \\ (J - N)(J - N + 1),\ i = N, \end{cases} \qquad (9)$$

and

$$\gamma = \frac{1}{N}[\sqrt{\lambda_n T' + \mu \ln(J)} - \sqrt{\lambda_n T'}]^2. \qquad (10)$$

Notice that as $\lambda_n \rightarrow 0$, $\gamma \rightarrow \lambda_s \tau$ and (8) becomes a bound to the exact error-probability in (4)-(6). Although the second sum on the right-hand side of (8) can be summed analytically, we did not do so because it provides no further insight.

Figures (2) and (3) show for the quantum-limited case the symbol error-probability as a function of signal energy μ in photons/nat, the index of overlap N and the PPM alphabet size Q. Similar results for the background noise case with one noise photon per slot, $\lambda_n T' = 1$, are shown in figures (4) and (5). These results were obtained by using the bound with the Q-function in equation (8) which is tighter than the Chernoff bound. It was found that the Chernoff bound in (8) is about 0.5 dB away from the results presented in figures 3 and 4.

The significant degradation in performance with increasing overlap N is obvious from the figures. As an example, for quantum-limited channels with $Q = 2$ and an error-probability of 10^{-6} there is about 1.8, 3.0, and 3.8 dB degradation in going from $N = 1$ to $N = 3$, 5, and 7 respectively. The coresponding losses from overlap for $Q = 4$ are 2.8, 4.0, and 5.1 dB respectively, indicating a higher loss with overlap as Q is increased. Similar results for the background noise case are 1.2, 2.2 and 2.9 dB loss for $Q = 2$ and 1.7, 2.9 and 3.8 for $Q = 4$. These losses are significantly less than those reported in [3] for a suboptimal receiver. The gain in allowing overlap is of course an increase in throughput by a factor $p = \ln(J)/\ln(Q)$ as compared to conventional Q-ary PPM. The index of overlap needed

to achieve a p-fold increase in throughput is $N = (Q^p - 1)/(Q - 1)$, which increases exponentially with p. Also clear from figures 2-5 is the fact that increasing Q improves performance for the same overlap N and signal level μ. The price paid in this case is an increased bandwidth since increasing Q increases the number of dimensions in the signal space.

A comparison between the performance of the optimal receiver in figures 3 and 5 to the performance of the suboptimal receiver studied in [3] for $Q = 4$ indicates that the latter is significantly inferior, especially for large indexes of overlap N. For example, for the quantum-limited channel and an error-probability of 10^{-7} the suboptimal receiver in [3] is about 3 dB inferior for $N = 3$ and about 4.5 dB inferior for $N = 4$. Similarly, for the background noise case the difference between the optimal and suboptimal receivers is at least 3.5 dB for $N = 4$ and at least 4.1 dB for $N = 5$.

In the next section we will show how the use of trellis-coded modulation can result in a doubling in throughput at no performance loss.

III. SOME IMPLICATIONS OF TCM

A. The Distance Metric

In presenting the results in this section we assume that the reader is familiar with Ungerboeck's work on trellis-coded modulation [1]. Tutorial versions of [1] that are easy to follow can be found in [6] and [7].

The first step involved in applying the ideas of TCM to the optical channel is to identify a distance metric that will be used for partitioning the OPPM signal set. To facilitate the search for such a metric we will refer to the OPPM symbol with a pulse starting at time $t_j = (j-1)\tau$ as symbol j for $j = 1, 2, \cdots, J$. This definition is illustrated in figure 1 for $Q = 2$, $N = 3$ and $J = 4$. What we are interested in obtaining is a function $f(j,k)$ between *symbols* j and k such that, given for example that j was sent, the probability of confusing j for k is a monotonically non-increasing function of $f(j,k)$, $j,\ k = 1, 2, \cdots, J$. More generally, we need to show that the probability of choosing a given incorrect *path* in the trellis is a monotonically non-increasing function of the distance between the incorrect and

correct paths. In the next few lines we first find a metric that satisfies our requirements between symbols and then show that it is valid between paths as well.

A function satisfying our requirements between symbols can be easily identified by recalling equation (7B) in appendix B which represents a Chernoff bound to the above mentioned probability, i.e.,

$$Pr[N_j \leq N_k/j] \;\leq\; \exp[-\frac{\delta_{jk}}{N}(\sqrt{\lambda_n T' + \mu R \ln(J)} \;-\; \sqrt{\lambda_n T'})^2] \tag{11}$$

where

$$\delta_{jk} \;=\; \begin{cases} |j \;-\; k|, & \text{if } |j \;-\; k| \leq N; \\ N, & \text{if } |j \;-\; k| > N. \end{cases} \tag{12}$$

We remind the reader that N_j and N_k are the number of counts observed in the $j-th$ and $k-th$ symbol subintervals respectively. Notice that the probability of deciding k when j was sent on the left-hand side of (11) is monotonically non-increasing with δ_{jk} which satisfies our condition for a distance metric (notice also that δ_{jk} is indeed a metric). A simple proof presented in appendix C shows that the above metric is valid also for paths in the trellis as required above.

As a final point before proceeding, we note that δ_{jk} can be used to partition the OPPM signals in sets with increasing distance but it cannot be used to compare the performance of OPPM systems with different index of overlap N. A more proper distance measure in this case is the whole exponent in equation (11). A simple study of this exponent shows that it decreases monotonically with N although not quite in an inverse relation because of the dependence of J on N. In the sequel we will use the above metric in set partitioning and in deriving probability of error expressions when coding is used.

Having identified a metric, we are now ready to show how TCM can be used for the optical channel to improve performance.

B. Improving Throughput

Let us consider the problem of doubling the throughput of a binary ($Q = 2$) PPM system by allowing overlap. This can be accomplished at no bandwidth expansion with an overlap $N = 3$ at the cost, however, of performance. Instead, we use an index of overlap

$N = 7$ which results in tripling the throughput and then use a rate 2/3 trellis code on the expanded signal set to trade-off some of the throughput gain for performance. As our rate 2/3 code we use the simple four-state code described by Ungerboeck [6] whose trellis diagram is repeated in figure 6 for convenience. In order to partition the signal set in subsets with increasing distance, we use the distance metric δ_{jk} discussed above. Figure 7 shows the results of the set partitioning.

The minimum free distance of the code is easily seen to be between parallel transitions with $\delta_{free} = 4$; the number of neighbors at this distance is one. Notice that although we are using the same code as in [6], because of the different distance metric and the fact that OPPM is not completely symmetric the minimum free distance may be achieved by some path other than when phase-shift keying (PSK) is used with a Euclidean distance metric. An example of this will be seen later in this section.

Approximating the error-probability by the error-event probability, we have for high signal levels and the quantum limited channel

$$P(\epsilon) \approx \frac{1}{2}\exp[-\delta_{free}\frac{R\ln(J)}{N}\mu] = \frac{1}{2}\exp[-\frac{8\ln(8)}{21}\mu]. \quad (13)$$

Equation (13) expresses the fact that errors can be made only if no counts are detected in the four slots of the signal interval that do not overlap with the other symbol in a parallel transition. For uncoded binary PPM we have

$$P(\epsilon) = \frac{1}{2}\exp[-\ln(2)\mu]. \quad (14)$$

Comparing (13) and (14) we observe a modest 0.6 dB gain with our simple coding scheme obtained, however, at twice the throughput compared to binary PPM. For the background noise case with $\lambda_n T' = 1$ we have for the coded case and using the Chernoff bound in (11) for comparison

$$P(\epsilon) < \exp[-\frac{\delta_{free}}{N}(\sqrt{\lambda_n T' + R\ln(J)\mu} - \sqrt{\lambda_n T'})^2] = \exp[-\frac{4}{7}(\sqrt{1+\frac{2}{3}\ln(8)\mu} - 1)^2] \quad (15)$$

and for uncoded binary PPM

$$P(\epsilon) \leq \exp[-(\sqrt{\lambda_n T' + \ln(Q)\mu} - \sqrt{\lambda_n T'})^2] = \exp[-(\sqrt{1+\ln(2)\mu} - 1)^2]. \quad (16)$$

A brief comparison of equations (15) and (16) shows that even after doubling throughput there is, at an error-probability of 10^{-6}, about a 1.0 dB advantage with the coded system as compared to uncoded binary PPM. Asymptotically as $\mu \rightarrow \infty$, ($P(\epsilon) \rightarrow 0$) the gain reduces to the same level as for the quantum-limited channel, as expected. Finally, the bounds indicate that for any finite number of photons/nat, the gain increases with increasing number of average noise counts.

Let us now consider the same problem of doubling the throughput using the eight-state trellis code that was introduced in [1] for 8-PSK. The trellis for this code is repeated in figure 8 which shows the path with the minimum distance from the all one path. Notice that whereas for the PSK case [1] there are two paths at the same minimum (Euclidean) distance, in our case there is only one and it is at $\delta_{free} = 5$ from the all one path. This distance should be compared with the $\delta_{free} = 4$ distance for the 4-state code, a gain of about 1 dB over the results reported above.

C. Improving Performance

If the objective is to improve performance without a bandwidth expansion, the examples that follow show that this can be accomplished with OPPM for the optical channel using the same codes that Ungerboeck derived for the Gaussian channel.

Let us compare the performance of the coded system with $N = 7$, $Q = 2$, given by (13), to an uncoded system with $N = 3$ and $Q = 2$. Both systems require the same bandwidth and have the same throughput. Using equation (4) for a quantum-limited system to compute the error-probability for the uncoded system, we see that the coded quantum-limited system in (13) is about 2.5 dB superior at an error-probability of 10^{-6}. A similar comparison for systems with background noise using the Chernoff bounds in equations (8) and (15) indicates a gain of about 2.2 dB with coded systems. This gain approaches asymptotically for large signal levels the gain achieved by quantum-limited systems. As a final example, it can be shown that about a 3.5 dB gain over uncoded binary PPM can be achieved with the rate 2/3 code whose trellis is shown in figure 6. In this case no parallel transitions are necessary.

For the 8-state code of figure 8, about an extra 1 dB gain is achieved over uncoded systems.

Before we end this section, we briefly describe the decoder for completeness.

D. Decoding of Coded OPPM

The sufficient statistic for symbol decisions for both the quantum-limited as well as the background noise limited channels is, as noted earlier, the number of counts observed in the J subintervals corresponding to possible pulse-positions. In the sequel we will denote a sequence of L symbols transmitted by the encoder by a set of indexes $\{ j_i \}$, $i = 1, 2, \cdots, L$ where $j_i \in \{1, 2, \cdots, J\}$. For sequence estimation, a maximum-likelihood (ML) decoder maximizes over the set of all possible sequences allowed by the encoder the following statistic

$$\ell(\{j_i\}) = \sum_{i=1}^{L} N_{j_i}. \tag{17}$$

Soft-decision decoding for the trellis codes discussed above is accomplished in two steps when parallel transitions exist, as described by Ungerboeck: in the first step the symbol with the largest number of counts is found among symbols in parallel transitions. Both the symbol and its number of counts are retained. In the second step, the Viterbi algorithm is used to find the best path in the trellis that maximizes (17), using as path metric the accumulated number of counts for each path. Equal counts are resolved arbitrarily.

IV. CONCLUSIONS

The performance of both coded and uncoded overlapping PPM systems has been investigated for the optical direct-detection channel. To facilitate set partitioning, a simple distance metric was derived which was shown to be valid for the optical channel. Using simple trellis codes over an expanded OPPM signal set, it was shown that both a throughput and a performance gain can be achieved with simple codes and no bandwidth expansion. The trellis-codes used where among those introduced by Ungerboeck and are optimal for the Gaussian channel and a Euclidean distance metric. Although a performance gain was obtained using these codes for the optical channel, it is not clear that they are optimal for

this channel and the distance metric derived herein.

V. REFERENCES

1. G. Ungerboeck, "Channel Coding With Multilevel/Phase Signals," IEEE Transactions on Information Theory, Vol. IT-28, pp.55-67, January 1982.

2. I. Bar-David and G. Kaplan, "Information Rates of Photon Limited Overlapping Pulse Position Modulation Channels," IEEE Transactions on Information Theory, Vol. IT-30, pp. 455-464, May 1984.

3. G.M. Lee and G.W. Schroeder, "Optical Pulse-Position Modulation with Multiple Positions per Pulsewidth," IEEE Transactions on Communications, Vol. COM-25, pp. 360-364, March 1977.

4. R.J. McEliece, "Practical Codes for Photon Communications," IEEE Transactions on Information theory, Vol. IT-27, pp. 393-397, July 1981.

5. J.L. Massey, "Capacity, Cutoff-Rate and Coding for a Direct-Detection Optical Channel," IEEE Transactions on communications, Vol. COM-29, pp. 1616-1621, November 1981.

6. G. Ungerboeck, "Trellis Coded Modulation with Redundant Signal Sets Part I: Introduction," IEEE Communications Magazine, Vol. 25, pp. 5-11, February 1987.

7. G. Ungerboeck, "Trellis Coded Modulation with Reduntant Signal Sets Part II: State of the Art," IEEE Communications Magazine, Vol. 25, pp. 12-21, February 1987.

8. N.L. Johnson, "On an extension of the connection between Poisson and chi-square distribution," Biometrika, Vol. 46, pp. 352-364, 1959.

9. J.I. Marcum, "A Statistical Theory of Target Detection by Pulsed Radar: Mathematical Appendix," IRE Transactions on Information Theory, Vol. IT-6, pp. 59-267, April 1960.

AKNOWLEDGEMENT

I would like to thank my colleagues Dr. Pierce Cantrell for supplying the Fortran routine to compute the Q-function and Dr. Tom Fischer for some interesting discussions.

FIGURE CAPTIONS

Figure 1. An Example of OPPM with Q=2, N=3, J=4.

Figure 2. Uncoded Error-Probability for OPPM and Q=2 as a Function of Overlap and Photons/nat: Quantum-Limited Case.

Figure 3. Uncoded Error-Probability for OPPM and Q=4 as a Function of Overlap and Photons/nat: Quantum-Limited Case.

Figure 4. Uncoded Error-Probability for OPPM and Q=2 as a Function of Overlap and Photons/nat: Background Noise Case.

Figure 5. Uncoded Error-Probability for OPPM and Q=4 as a Function of Overlap and Photons/nat: Background Noise Case.

Figure 6. Trellis for the Four-State Code.

Figure 7. Set Partitioning of OPPM with Q=2, N=7, J=8.

Figure 8. Trellis for Eight-State Code.

APPENDIX A

Derivation of Equations (4)-(6)

We first note that the probabilities of making a correct decision given that the first or the $J-th$ symbol was sent are the same. We call this probability P_1. Similarly, the probability of making a correct decision, call it P_2, given that any of the other $(J-2)$ symbols was sent is the same. Under these observations, equation (4) is evident.

Let us compute P_1 first. Assuming that symbol 1 was sent, only the slots $1, 2, \cdots, N$ may have non-zero counts. If slot 1 has nonzero counts, an event that happens with probability $(1-\epsilon)$, then a correct decision is made with probability one. If slot 1 is erased *and* slot 2 has nonzero counts, which happens with probability $\epsilon(1-\epsilon)$, then there is $1/2$ probability of choosing the right symbol between the two candidates 1 and 2. Similarly, if slots 1 *and* 2 are erased, *and* 3 is not, which occurs with probability $\epsilon^2(1-\epsilon)$, then there is $1/3$ probability of making a correct choice. Applying this reasoning to other slots and noting that if *all* N slots are erased, then a random choice among the J symbols is made, we obtain equation (5).

To compute P_2 we use similar arguments as above.

APPENDIX B

Derivation of Equation (8)

The error probability is given by

$$P(\epsilon) = \frac{1}{J}\sum_{j=1}^{J} P(\epsilon/j) \tag{1B}$$

where $P(\epsilon/j)$ is the probability of error given that symbol j was sent. Assuming pessimistically that in the case of equal symbol counts between the correct symbol and some other symbol a wrong decision is made, we have

$$P(\epsilon) \leq Pr[\bigcup_{k \neq j} \{N_j \leq N_k\}/j] \leq \sum_{k \neq j} Pr[N_j \leq N_k/j]. \tag{2B}$$

The second inequality above is justified by the union bound. Focusing on the probabilities on the right-hand side of (2B) we have after a little thought

$$Pr[N_j \leq N_k/j] = Pr[N'_j \leq N'_k] \tag{3B}$$

where N'_j and N'_k are independent Poisson random variables with means $\frac{\delta_{jk}}{N}(\lambda_n + \lambda_s)T'$ and $\frac{\delta_{jk}}{N}\lambda_n T'$ respectively and

$$\delta_{jk} = \begin{cases} |j - k|, & \text{if } |j - k| \leq N \\ N, & \text{if } |j - k| > N. \end{cases} \tag{4B}$$

Equations (3B) and (4B) can be easily derived by noting that between symbols j and k there is an overlap of $(N - |j - k|) \geq 0$ and that the symbols become orthogonal (no overlap) when $|j - k| > N$.

It follows from (3B) and (4B) that [8]

$$Pr[N_j \leq N_K/j] = Q_1[\sqrt{\frac{2\lambda_n T' \delta_{jk}}{N}}, \sqrt{\frac{2\delta_{jk}(\lambda_n + \lambda_s)T'}{N}}] \tag{5B}$$

where

$$Q_1(\alpha, \beta) = \exp(-\frac{\alpha^2 + \beta^2}{2})\sum_{k=0}^{\infty}(\frac{\beta}{\alpha})^k I_k(\alpha\beta) \tag{6B}$$

is Marcum's Q-function [9]. A final simplification can be made by using a Chernoff bound to the probability in (5B) to yield

$$Pr[N_j \leq N_k] \leq \exp[-\frac{\delta_{jk}}{N}(\sqrt{\lambda_n T' + \lambda_s T'} - \sqrt{\lambda_n T'})^2]. \qquad (7B)$$

Combining equations (1B), (2B), (5B) and (7B) we obtain

$$\begin{aligned} P(\epsilon) &\leq \frac{1}{J}\sum_{j=1}^{J}\sum_{k\neq j} Q_1[\sqrt{\frac{2\delta_{jk}\lambda_n T'}{N}}, \sqrt{\frac{2\delta_{jk}(\lambda_n + \lambda_s)T'}{N}}] \\ &\leq \frac{1}{J}\sum_{j=1}^{J}\sum_{k\neq j} \exp[-\frac{\delta_{jk}}{N}(\sqrt{(\lambda_n + \lambda_s)T'} - \sqrt{\lambda_n T'})^2]. \end{aligned} \qquad (9B)$$

Equation (9B) can be simplified further by noting that $\delta_{jk} \in \{1, 2, \cdots, N\}$ when $j \neq k$. Denoting by $a(i)$ the number of times $\delta_{jk} = i$, it can be shown that

$$a(i) = \begin{cases} 2(J - i), & i = 1, 2, \cdots, (N-1) \\ (J-N)(J-N+1), & \text{i=N.} \end{cases} \qquad (10B)$$

Substituting (10B) in (9B) we obtain equation (8).

APPENDIX C

Validation of the Distance Metric

Here we show that the distance metric δ_{jk} is valid also for paths and thus it is a valid metric.

Consider a sequence of L symbols in the trellis corresponding to the transmitted (correct) path. The decision statistic for this path is the sum, call it ℓ_0, of counts in each of the symbol intervals in the path. If we describe the correct path by the sequence of symbols $(j_1, j_2, \cdots, j_L)$ where $j_i \in \{1, 2, \cdots, J\}$, we have

$$\ell_0 = \sum_{i=1}^{L} N_{j_i} . \tag{1C}$$

Now consider another path through the trellis other than the correct path described by $(k_1, k_2, \cdots, k_L)$ with a decision statistic ℓ_1,

$$\ell_1 = \sum_{i=1}^{L} N_{k_i} . \tag{2}$$

The probability that an erroneous decision will be made between the above two paths is bounded from above by the probability that ℓ_0 is less than or equal to ℓ_1, i.e.,

$$P(\epsilon) \leq Pr[\sum_{i=1}^{L} (N_{j_i} - N_{k_i}) \leq 0]. \tag{3C}$$

In general when the two symbols corresponding to counts N_{j_i} and N_{k_i} overlap, the Poisson random variables N_{j_i} and N_{k_i} are not independent. However, we can write

$$(N_{j_i} - N_{k_i}) = (X_{j_i} - X_{k_i})$$

where X_{j_i} and X_{k_i} are independent Poisson random variables with means $\frac{\delta_{j_i k_i}}{N}(\lambda_n + \lambda_s)T'$ and $\frac{\delta_{j_i k_i}}{N}\lambda_n T'$ respectively. Here $\delta_{j_i k_i}$ is the distance between symbols j_i and k_i as defined in section III. The implications of the above arguments is that we can write $P(\epsilon) \leq Pr[X_0 \leq X_1]$ where $X_0 = \sum_{i=1}^{L} X_{j_i}$ and $X_1 = \sum_{i=1}^{L} X_{k_i}$ are independent Poisson variables with means

$$(\lambda_n + \lambda_s)\frac{T'}{N}\sum_{i=1}^{L} \delta_{j_i k_i}$$

and

$$\frac{\lambda_n T'}{N} \sum_{i=1}^{L} \delta_{j_i k_i}$$

respectively.

Using the Chernoff bound to further bound $P(\epsilon)$, we see that this probability is monotonically non-increasing with the distance between the correct and the incorrect paths given by $\sum_{i=1}^{L} \delta_{j_i k_i}$. Thus we have shown that the distance metric defined in section III. is valid also between paths.

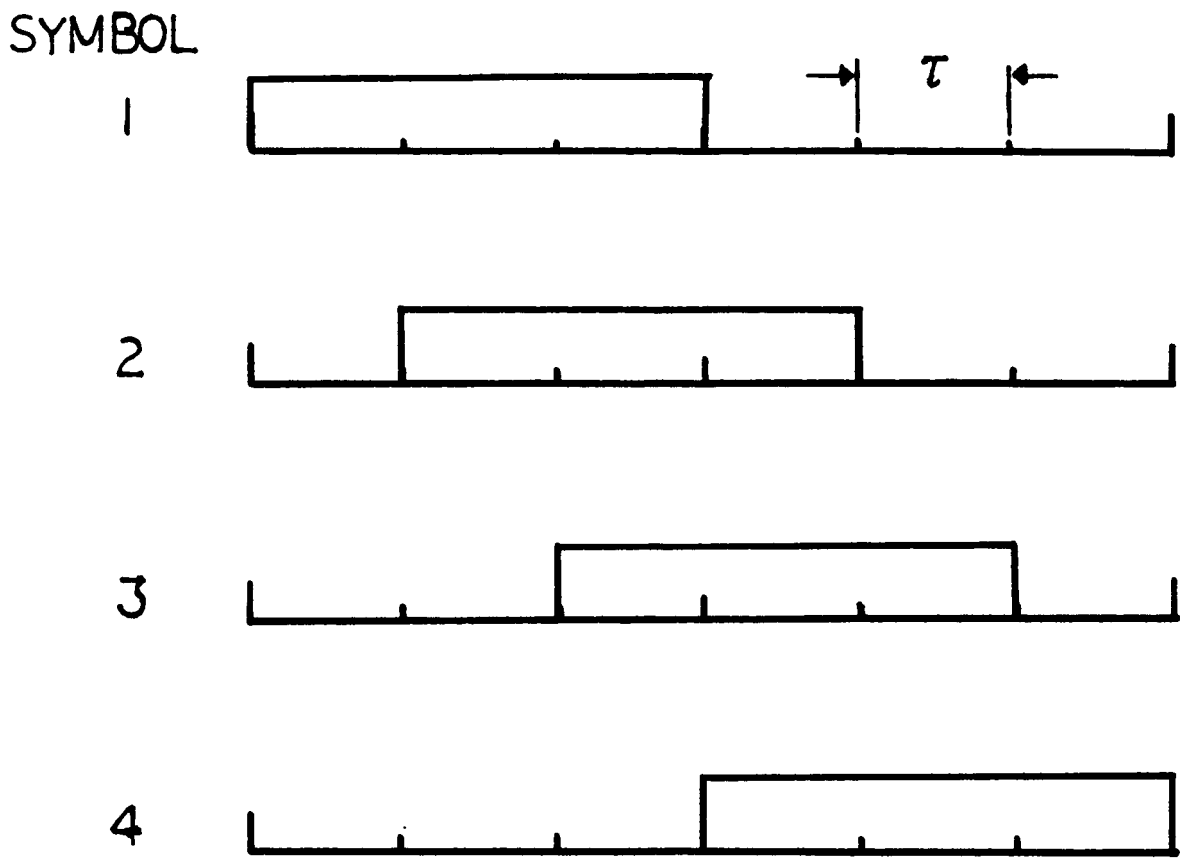

Figure 1. An Example of OPPM with Q=2, N=3, J=4.

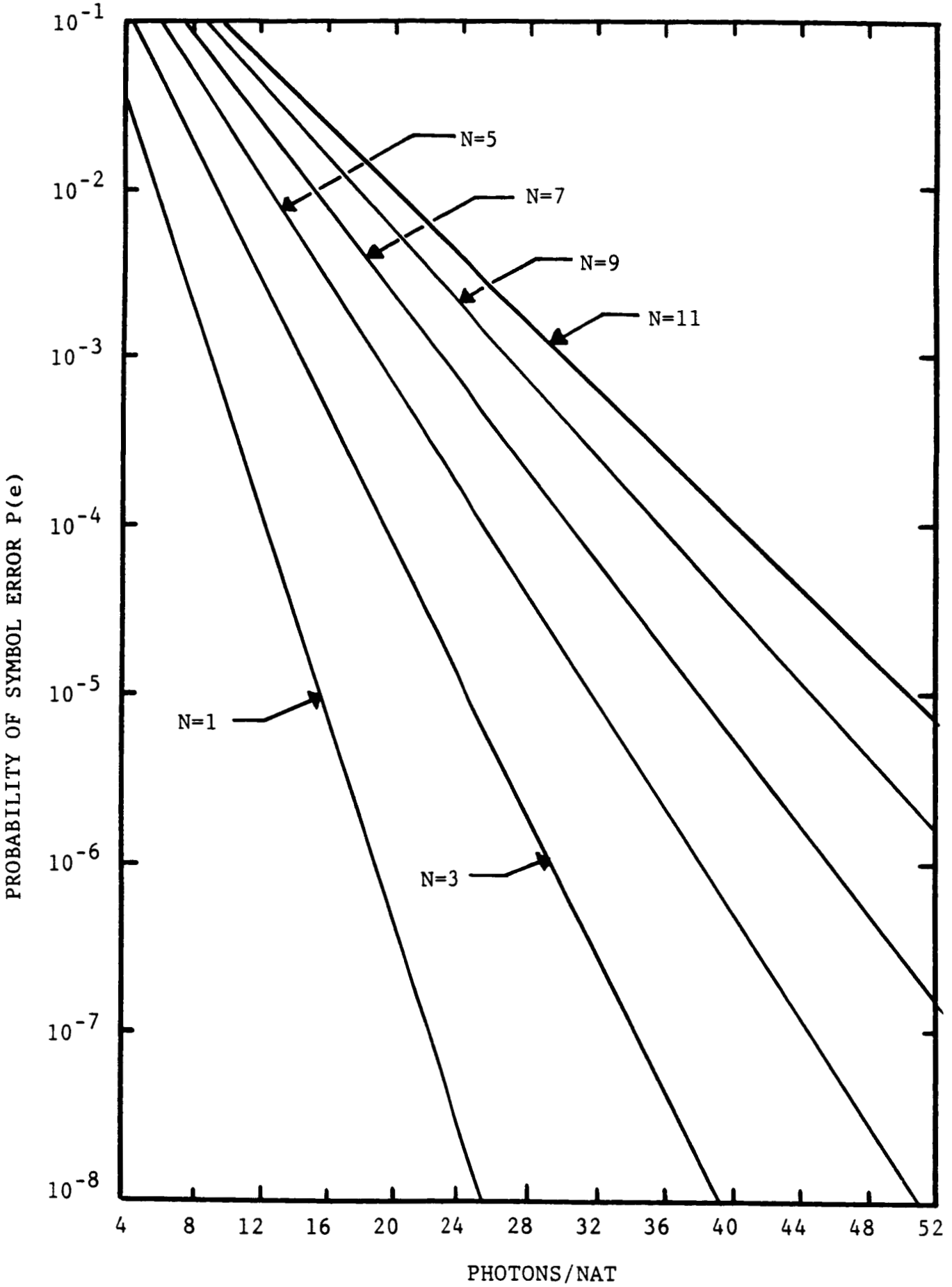

Figure 2. Uncoded Error-Probability for OPPM and Q=2 as a Function of Overlap and Photons/nat: Quantum-Limited Case.

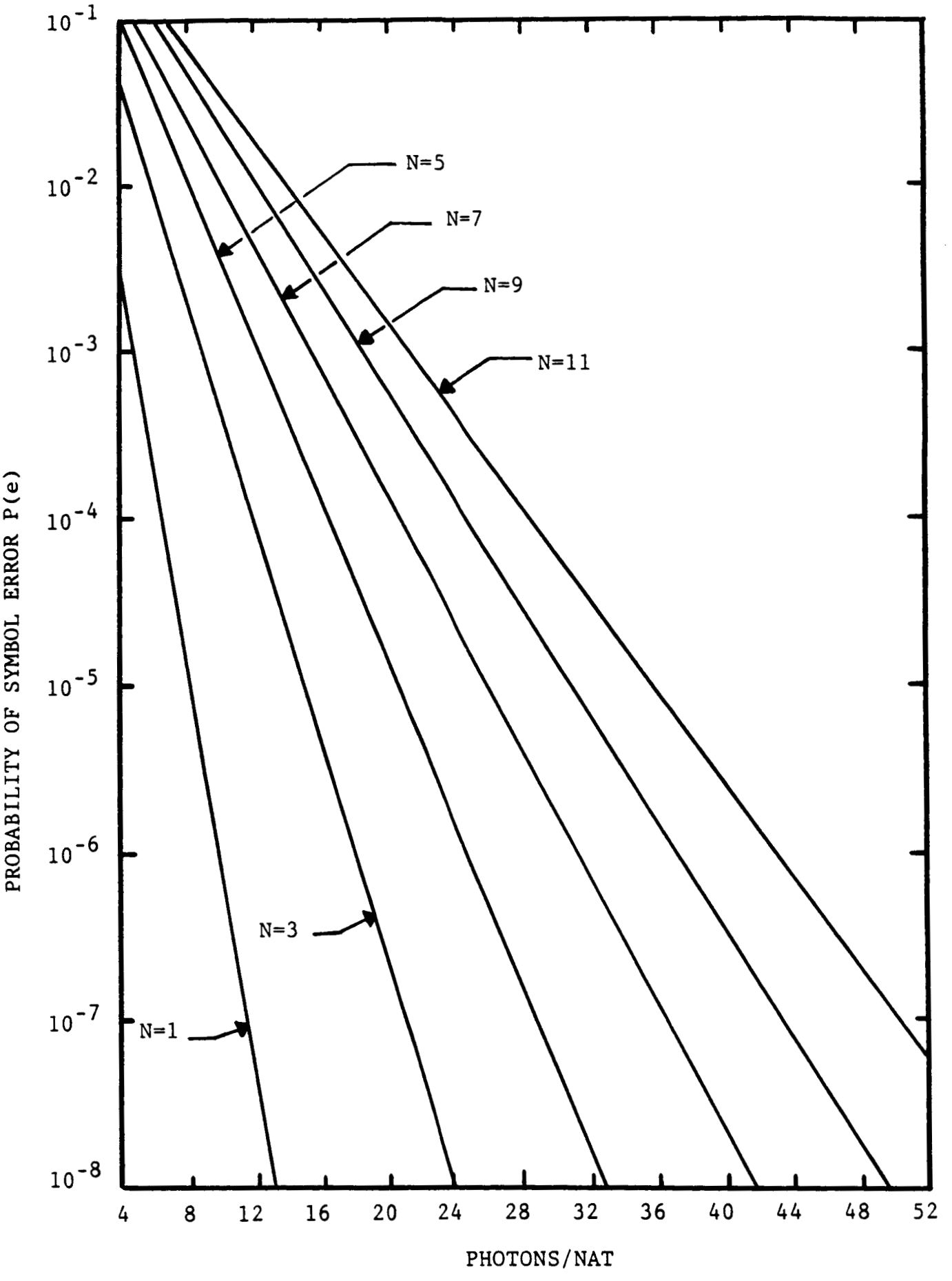

Figure 3. Uncoded Error-Probability for OPPM and Q=4 as a Function of Overlap and Photons/nat: Quantum-Limited Case.

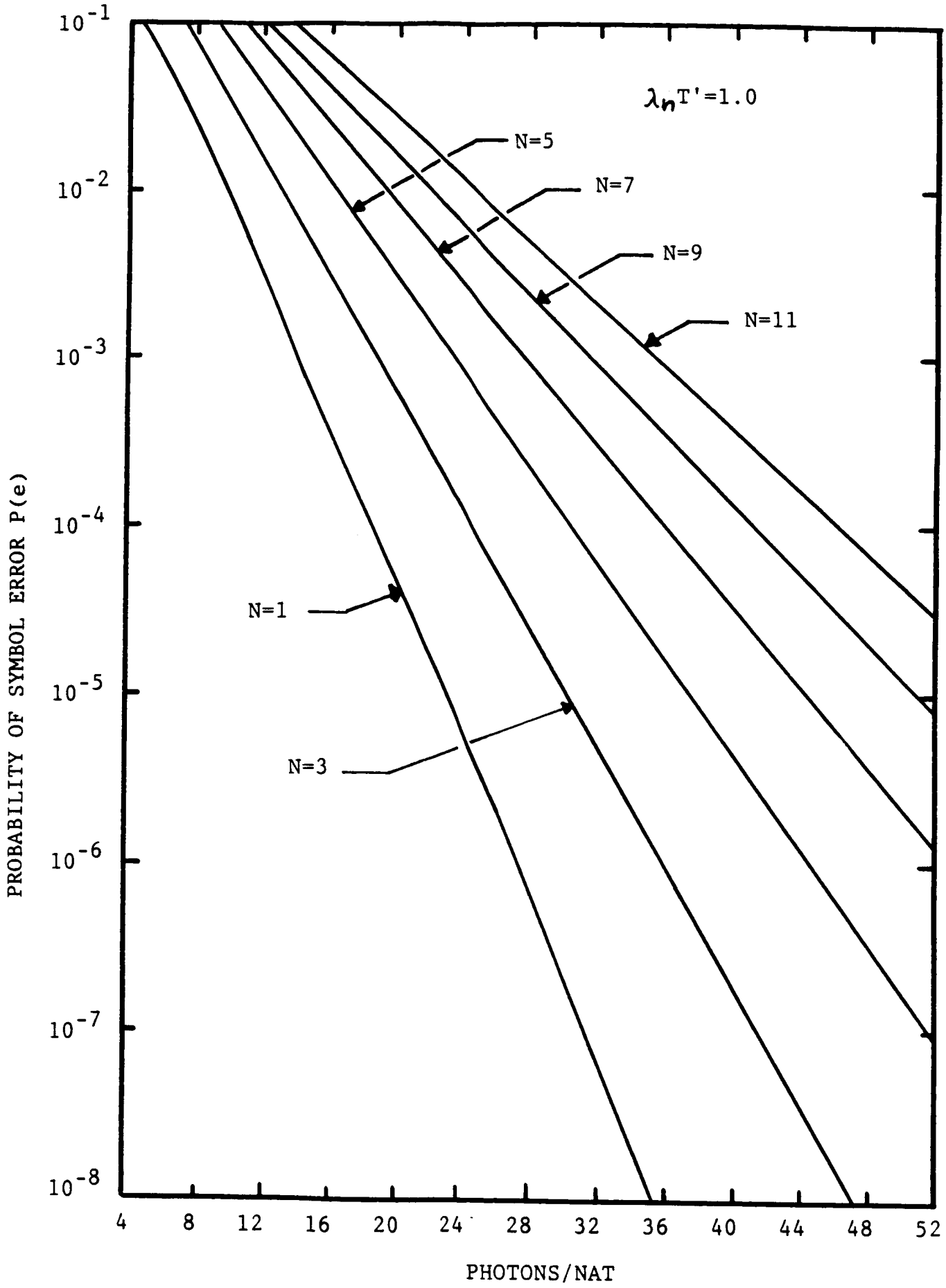

Figure 4. Uncoded Error-Probability for OPPM and Q=2 as a Function of Overlap and Photons/nat: Background Noise Case.

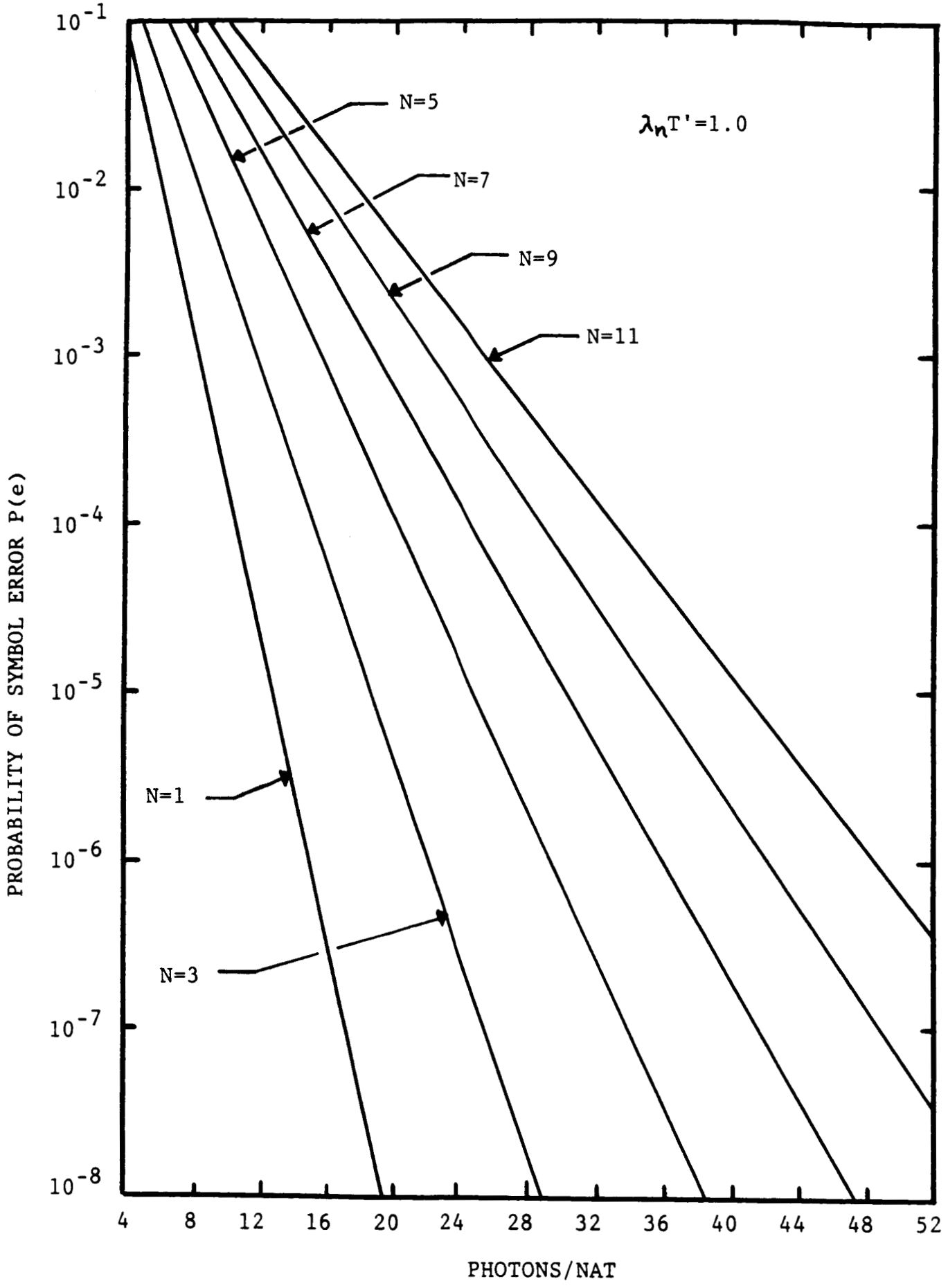

Figure 5. Uncoded Error-Probability for OPPM and Q=2 as a Function of Overlap and Photons/nat: Background Noise Case.

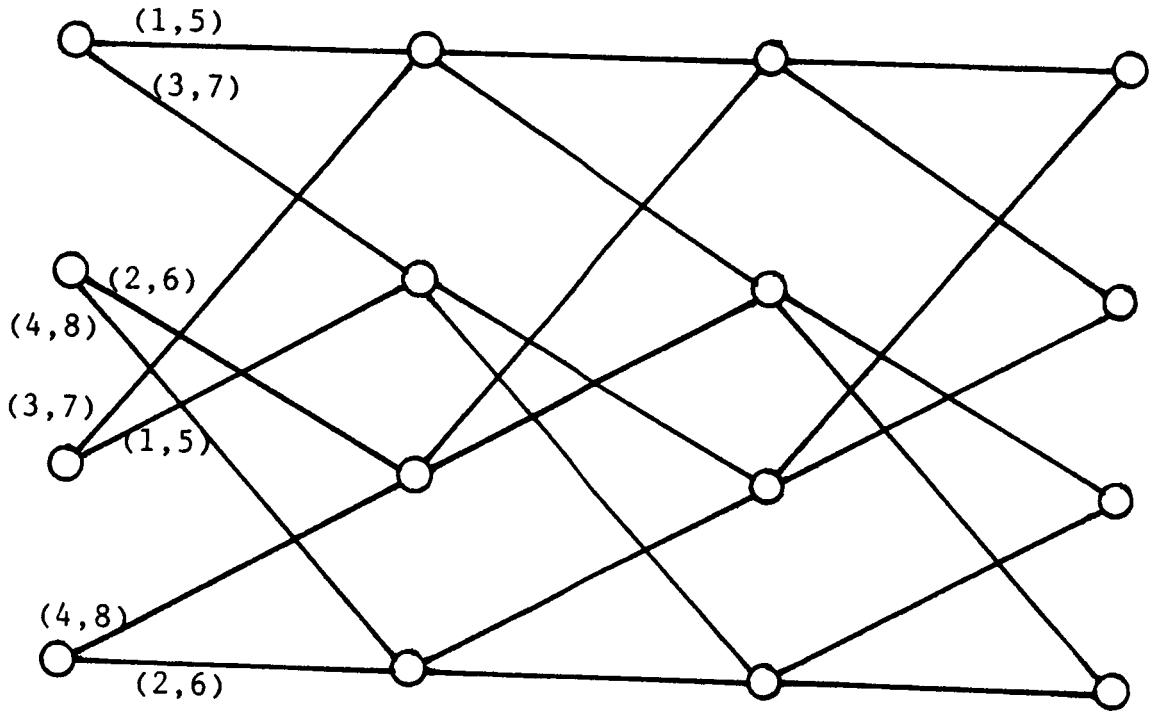

Figure 6. Trellis for the Four-State Code.

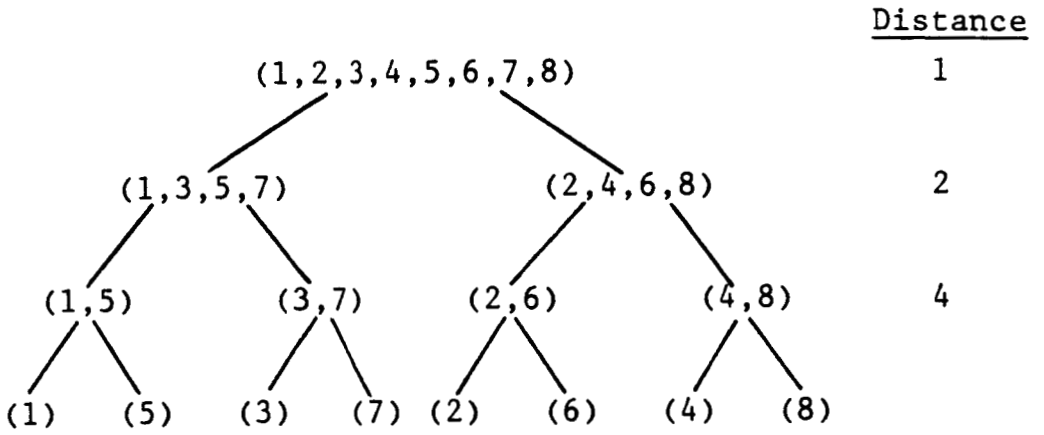

Figure 7. Set Partitioning of OPPM with Q=2, N=7, J=8.

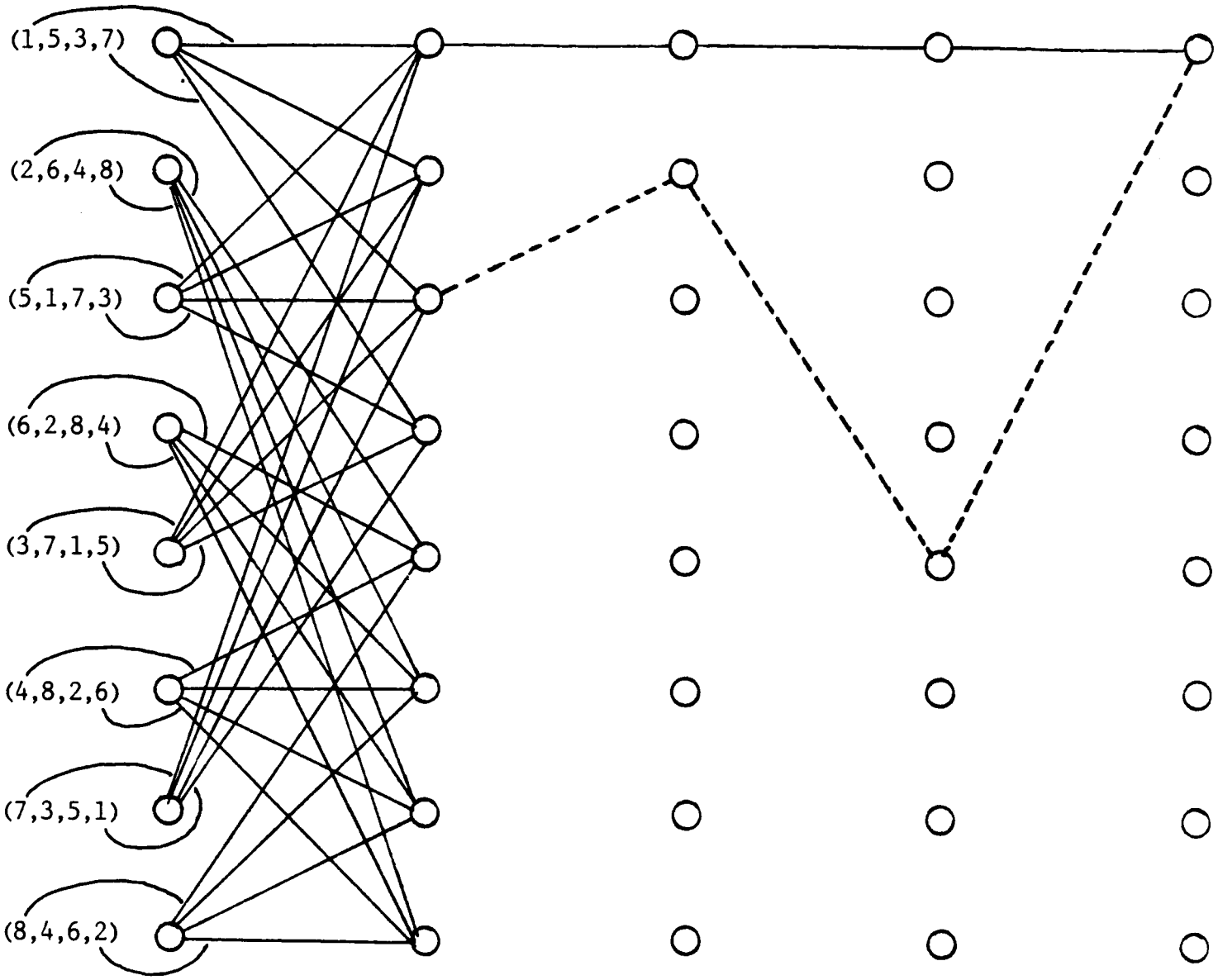

Figure 8. The Trellis for the Eight-State Code.

III. ABSTRACTS OF PREVIOUS REPORTS

In this section we include the abstracts of previous reports and papers that briefly describe the derived results. Complete versions of these reports and preprints accompany this final report.

A CASCADED CODING SCHEME FOR ERROR CONTROL AND ITS PERFORMANCE ANALYSIS *

Shu Lin
Texas A&M University
College TX 77843

Tadao Kasami, Tohru Fujiwara, Toyoo Takata
Osaka University
Toyonaka, Osaka, Japan

ABSTRACT

In this paper, we investigate a coding scheme for error control in data communication systems. The scheme is obtained by cascading two error-correcting codes, called the inner and outer codes. The error performance of the scheme is analyzed for a binary symmetric channel with bit-error rate $\epsilon < 1/2$. We show that, if the inner and outer codes are chosen properly, extremely high reliability can be attained even for a high channel bit-error rate. Various specific example schemes with inner codes ranging from high rates to very low rates and Reed-Solomon codes as outer codes are considered, and their error probabilities are evaluated. They all provide extremely high reliability even for very high bit-error rates, say 10^{-1} to 10^{-2}. Several example schemes are being considered by NASA for satellite and spacecraft down-link error control.

* This research was partially supported by NASA Grant No. NAG 5-778

A CASCADED CODING SCHEME FOR ERROR CONTROL AND ITS PERFORMANCE ANALYSIS*

Tadao Kasami, Tohru Fujiwara,
and
Toyoo Takata
Osaka University
Toyonaka, Osaka, Japan

Shu Lin
Department of E.E.
Texas A&M University
College Station, Texas 77843

ABSTRACT

In this paper, we investigate a coding scheme for error control in data communication systems. The scheme is obtained by cascading two error-correcting codes, called the inner and outer codes. The error performance of the scheme is analyzed for a binary symmetric channel with bit-error rate $\epsilon < 1/2$. We show that, if the inner and outer codes are chosen properly, extremely high reliability can be attained even for a high channel bit-error rate. Several example schemes with Reed-Solomon codes as outer codes are considered, and their error performance is evaluated. They all provide extremely high reliability. One particular example scheme with a shortened triple-error-correcting BCH code as the inner code and a Reed-Solomon code with symbols from $GF(2^8)$ as the outer code is being considered by NASA for satellite or spacecraft down-link error control.

---

* This paper was partially presented at the 8th Conference on Information Theory and Its Applications, Nara, Japan, December 1985.

* This research is supported by NASA Grants No. NAG 5-407 and NAG 5-778.

TWO HYBRID ARQ ERROR CONTROL SCHEMES FOR NEAR EARTH SATELLITE COMMUNICATIONS *

Shu Lin
Department of E.E.
Texas A & M University
College Station, Texas 77843

Tadao Kasami
Faculty of Engineering Science
Osaka University
Toyonaka, Osaka, Japan 560

ABSTRACT

In this report, two hybrid ARQ error control schemes are proposed for NASA near earth satellite communications. Both schemes are adaptive in nature, and employ cascaded codes to achieve both high reliability and throughput efficiency for high data rate file transfer.

* This work was supported by NASA Grant No. NAG 5-778.

ON THE SYNCHRONIZABILITY AND DETECTABILITY OF RANDOM PPM SEQUENCES *

by

Costas N. Georghiades
Electrical Engineering Department
Texas A&M University
College Station, TX 77843

ABSTRACT

The problem of synchronization and detection of random pulse-position-modulation (PPM) sequences is investigated under the assumption of perfect slot synchronization. Maximum-likelihood PPM symbol synchronization and receiver algorithms are derived that make decisions based both on soft as well as hard data; these algorithms are seen to be easily implementable. We derive bounds on the symbol error probability as well as the probability of false synchronization that indicate the existence of a rather severe performance floor, which can easily be the limiting factor in the overall system performance. The performance floor is inherent in the PPM format and random data and becomes more serious as the PPM alphabet size Q is increased. A way to eliminate the performance floor is suggested by inserting "special" PPM symbols in the random data stream.

* This work was supported by NASA grant No. NAG 5-778

IV. ACKNOWLEDGEMENT

Professor Shu Lin and I would like to thank NASA for providing the funds to perform the research described herein.